ARTICLE

Indium(III)-terpyridine complexes: synthesis, structures and remarkable antifungal and anticancer activities

Xiao Chen,[a] Qinguo Zhang,[b] Ashley Kaswer, [a] Hyunjeong Kim,[a] Maisha Ahmed,[a] Michelle C. Neary,[c] Shu-Yuan Cheng, [a] Guoqi Zhang*[a] and Jason M. Rauceo*[a]

Complexes of non-radioactive indium(III) with 2,2´;6´,2´´-terpyridine (tpy) ligands are rarely explored despite the popularity of tpy as a strong chelating ligand backbone. Herein, three mononuclear indium(III) complexes (**In-1**, **In-2** and **In-3**) of tpy and its 4´-Cl and 4´-pyridyl derivatives have been synthesized and structurally characterized. While the crystal structure of **In-1** has been previously studied, **In-2** and **In-3** were isolated and characterized for the first time. Two different polymorphs of **In-2** were observed by simply varying the concentration of reactions. Molecules of **In-3** were determined by X-ray crystallography to adopt the same mononuclear coordination mode as found in **In-1** and **In-2**, while the remaining 4´-pyridyl ring was uncoordinated. Bioactivity studies revealed that indium(III) complexes **In-1**, **In-2**, and **In-3** were fungicidal against the human fungal pathogen, *Candida albicans*, and several non-albicans *Candida* species. Moreover, the cytotoxicity studies showed these compounds were remarkably antiproliferative against human breast cancer cells (MCF-7 and MDA-MB 468).

1 Introduction

Metal complexes of tpy have been extensively explored for decades because of their widespread applications in functional materials, supramolecular chemistry, catalysis, as well as anticancer, antibacterial and antifungal research.[1-6] Due to the presence of a strong N_3 chelating cavity in its structure, tpy is uniquely capable of forming coordination complexes with nearly all metal ions across the periodic table from main group to transition and rare-earth metals.[7,8] Moreover, its structure is rather easy to be modified on its three pyridinyl rings, in particular, at the 4´-position through a facile one-pot Kröhnke condensation.[9,10] Thus, rich coordination chemistry as well as versatile supramolecular structures and properties based on tpy and its derivatives are anticipated.

Compared to numerous reports on transition metal-tpy complexes, main group metal-tpy complexes are relatively underexplored. We have recently revealed the outstanding catalytic performance of simple tpy complexes of alkali metal (Li, Na and K) triethylborohydrides in epoxide ring-opening reactions.[11] We also demonstrated the unusual organometallic reactivity of tpy and its 4'-substituted derivatives upon complexation with organoaluminum(III),[12] highlighting its well-known one-electron reductive activity while being coordinated to main group metals. To continue our research efforts in group 13 coordination chemistry, we were interested in studying the structures and potential biological applications of indium(III) complexes with tpy-based ligands which remained almost unexplored. The only examples reported thus far include tpy-indium(III) trifluoride, trichloride and dimethyl complexes, and research was focused merely on their synthesis and structural data.[13-15]

a. Department of Sciences, John Jay College and PhD Program in Chemistry at the Graduate Center, The City University of New York, New York, NY 10019, USA
b. Hunter College High School, 71 E, 94th Street, New York, NY, 10128, USA
c. Department of Chemistry, Hunter College, The City University of New York, New York, NY 10065, USA

Although the study of biological applications of non-radioactive indium(III) complexes is still in its infancy, compared to radioactive [111]In(III) compounds that have been well explored, some indium(III) complexes have been known to display potential pharmacological applications.[16-20] In particular, indium(III) complexes with thiosemicarbazone ligands have shown notable antitumor, antimicrobial and antifungal activities.[21,22] As a popular organic ligand in coordination chemistry, tpy is also well-known for its strong intercalative interactions with DNA and hence has been utilized as an ideal metal chelator for preparation of metallic antiproliferative agents in numerous reports.[5,6,23,24] We envisioned that the combination of a tpy ligand and indium(III) ion would lead to observation of new bioactive molecules with potential pharmacological applications which have not yet been explored. Therefore, in this work we report on several indium(III) complexes of tpy and its 4'-substituted derivatives with a focus on their synthesis, structural analysis and biological properties, including antifungal and anticancer activities.
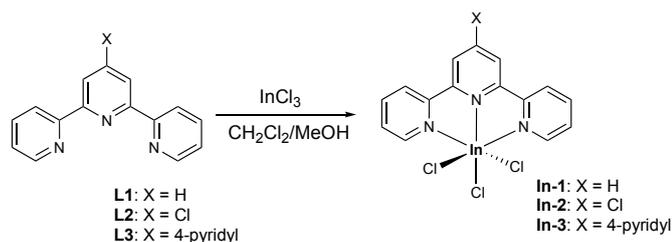

Scheme 1 Synthesis of indium(III) complexes with tpy-based ligands.

2 Results and discussion

2.1 Synthesis and crystal structures

The indium terpyridine complex **In-1** was synthesized by reacting equimolar 2,2';6',2''-terpyridine and $InCl_3$ salt in CH_2Cl_2-MeOH using a layering method, and colorless single-crystals were isolated. The structure was determined by X-ray crystallography to be identical to that reported previously.[13] Likewise, layering a solution of $InCl_3$ in MeOH onto a CH_2Cl_2-MeOH solution of 4'-Cltpy or 4'-pyridyltpy for two weeks led to the growth of X-ray quality crystals of complexes **In-2** and **In-3**, respectively. Both crystal structures are similar to that of **In-1**, consistent with the expected mononuclear chelating complex as shown in Scheme 1. It was interesting to find that complex **In-2** could crystallize as two different polymorphs (**In-2a** and **In-2b**) depending on the concentration of reactants during crystallization by layering (see Experimental section). **In-2a** crystallizes in the triclinic

space group *P-1*, while **In-2b** in the monoclinic $P2_1/c$. The molecular structures are shown in Fig. 1. In the unit cell of crystal **In-2a**, there exists one independent molecule of **In-2** and one cocrystallized methanol, while in **In-2b** two independent complexes were observed, along with three molecules of methanol. The relevant bond parameters are compared in Table 1, which shows only slight differences between the two polymorphs. Their geometrical parameters are also comparable to those found in **In-1**.[13] Due to the metal binding interactions, the tpy domain appears to be almost coplanar. Specifically, in structure **In-2a**, the angles between the least square planes of rings containing atoms N1 and N2, and N2 and N3 are 6.7(2) and 6.8(1)°, respectively. In structure **In-2b**, these angles are 4.8(2) and 6.3(2)°, respectively, for one independent molecule, and 5.3(2) and 6.0(2)° for the other. The discrepancy between the two polymorphs lies in their three-dimensional molecular packing patterns in the cell. In phase **In-2a**, the molecules of **In-2** packed in an alternating head-to-tail pattern with strong π···π stacking interactions between both the side and central pyridyl rings along the crystallographic *ab* axis (shown in Fig. 1B). The closest C···C contacts between the pyridyl rings are 3.306(2) and 3.367(2) Å, respectively. In contrast, the π···π stacking interaction in phase **In-2b** occurs between one side pyridyl ring and the central pyridyl ring of two adjacent molecules, although the molecules also adopt a head-to-tail arrangement along the crystallographic *a* axis. The shortest C···C distances for the π-stacking are 3.321(3) and 3.264(3) Å, respectively.
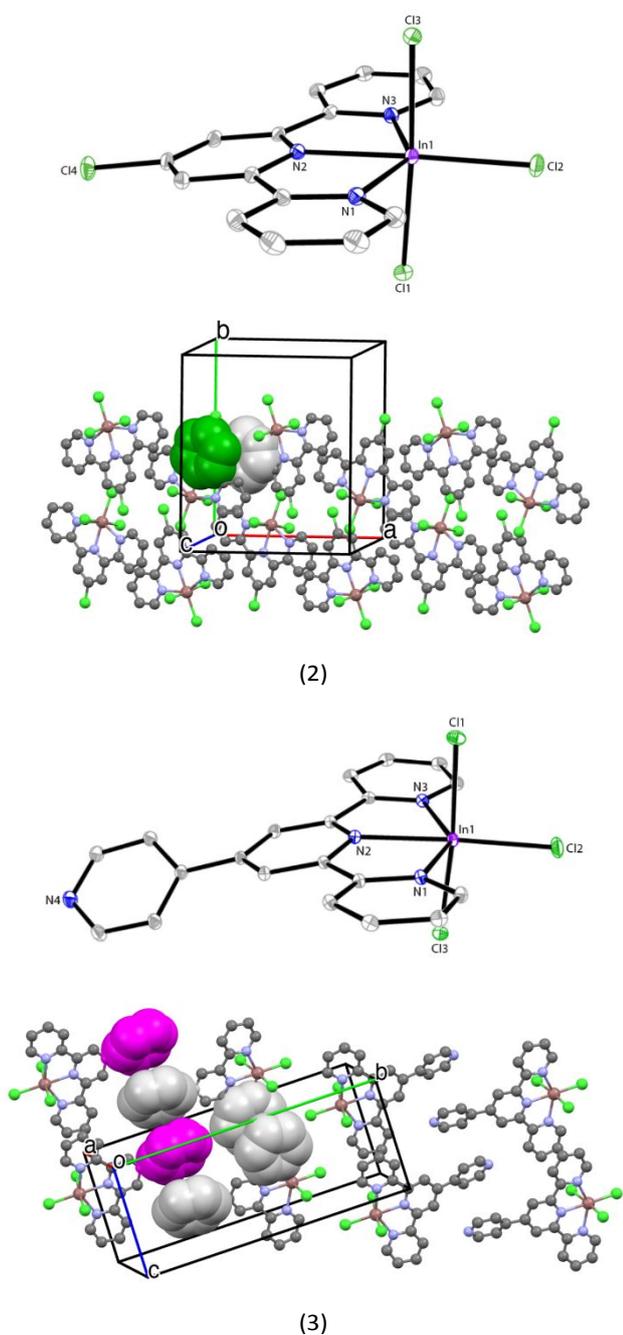

(1)

(2)

(3)
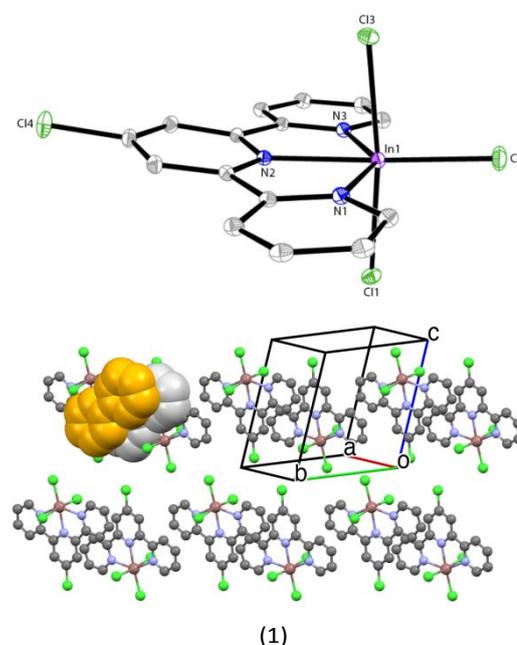
Fig. 1 The ORTEP presentation of cations for **In-2a** (1), **In-2b** (2) and **In-3** (3) with atomic displacement parameters drawn at the 30% probability level and their cell packing modes. Solvent molecules and H atoms are omitted for clarity.

Complex **3** was synthesized by the same procedure as for **In-2b**, and colorless plates of **In-3** were obtained by a layering method. Similar to **In-2b**, compound **In-3** also crystallizes in the monoclinic space group $P2_1/c$, yet there exists only one independent molecule of **In-3** in the asymmetric cell and no co-crystallized solvent molecules observed. The bond parameters

as listed in Table 1 are also comparable to those in **In-2a** and **In-2b**. Despite the presence of an additional 4'-pyridyl group on the tpy backbone as an extra coordination site that has often been involved in a coordination event with other metal ions to extend the molecular structures, the chelating coordination mode in **In-3** is found to be the same as that in **In-1** and **In-2**, leaving the 4'-pyridyl group uncoordinated. While maintaining a similar metal coordination environment for the three indium compounds, the tpy backbone in **In-3** is less coplanar that those found in **In-2a** and **In-2b**. It was found that in **In-3** the angles between the least square planes of rings containing atoms N1 and N2, and N2 and N3 are 10.8(2) and 9.9(2)°, respectively, much larger than the values for **In-2a** and **In-2b** (see above). This indicates the influence of 4'-substituents with various electronic and geometrical properties. In addition, the plane of 4'-pyridyl ring severely deviates from the tpy domain and the torsional angle between the least square planes of rings containing atoms N2 and N4 is 33.4(3)°. The intermolecular packing in **In-3** is also dominated by π···π stacking interactions. As presented in Fig. 1, two types of π-stacking modes have formed, *i.e.* the columnar packing between the 4'-pyridyl rings in a head-to-tail fashion along the crystallographic *c* axis and the offset stacking between the 'side-arm' 2-pyridyl rings from two adjacent complexes. The shortest intermolecular C···C distances for these two types of π-stacking are 3.367(3) and 3.320(2) Å, respectively.

Table 1 Selected geometrical parameters for **In-2a**, **In-2b** and **In-3** (Å and deg.).

	In-2a	In-2b	In-3
In1–N1	2.2586(10)	2.2793(16)	2.2687(14)
In1–N2	2.2602(10)	2.2554(15)	2.2567(15)
In1–N3	2.2771(9)	2.2801(16)	2.2749(15)
In2–N4		2.2751(16)	
In2–N5		2.2562(16)	
In2–N6		2.2781(16)	
In1–Cl1	2.4915(3)	2.4943(5)	2.4932(5)
In1–Cl2	2.3743(4)	2.3973(5)	2.3877(5)
In1–Cl3	2.5161(3)	2.4633(5)	2.4806(5)
In2–Cl5		2.4787(5)	
In2–Cl6		2.4150(5)	
In2–Cl7		2.4714(5)	
N2-In1–Cl1	88.33(3)	86.01(4)	89.85(4)
N2-In1–Cl2	176.31(3)	176.45(4)	177.15(4)
N5-In2–Cl5		84.38(4)	
N5-In2–Cl6		174.87(4)	

2.2 Antifungal activities for indium complexes

Indium(III)-thiosemicarbazone complexes exhibit antifungal properties against several *Candida* species including *Candida*

albicans, the most common human fungal pathogen.[21] Therefore, we hypothesized that indium(III)-tpy complexes that are unexplored may also demonstrate antifungal activity. Broth microdilution assays were performed to investigate the antifungal properties of indium complexes against various *C. albicans* strains and several non-a*lbicans Candida* species. The results of these growth tests are summarized on Table 2. Fluconazole, a known antifungal drug was included in the assay to validate the integrity of the strains, and the observed MICs are consistent with published findings.[25] Strikingly, indium(III)-tpy complexes **In-1**, **In-2** and **In-3** significantly inhibited growth of various *C. albicans* strains with MIC values ranging from 2 μg/mL to 16 μg/mL. Also, **In-1**, **In-2** and **In-3** inhibited growth of *C. glabrata*, *C. dubliniensis*, *C. parapsilosis*, and *C. tropicalis* with similar MICs to *C. albicans*. In all experiments **In-1** showed notably better performance than **In-2** and **In-3**. In contrast, the control experiments on the free ligands (L1-3) and InCl$_3$ salt reveal that except L1 and L2 which are moderately active against *C. albicans* SC5314 (MICs are 8 and 16 μg/mL, respectively), L3 and InCl$_3$ are both inactive (see Table S2, ESI).

Table 2 MIC (μg/mL) determination of indium(III)-tpy compounds against various *Candida* species.

Yeast strain	In-1	In-2	In-3	Fluconazole
C. albicans SC5314	2	4	16	2
C. albicans MC99	2	4	8	2
C. albicans MC102	2	4	16	2
C. albicans 3147	2	8	16	2
C. glabrata	0.5	4	4	1-2
C. tropicalis	2	8	16	1-2
C. parapsilosis	1	8	16	2
C. dubliniensis	1	4	8	2

To determine whether indium complexes are fungicidal, we cultured *C. albicans* SC5314 cells directly after MIC assays on nutrient solid media and counted colony forming units (CFUs). Our results show that **In-1**, **In-2** and **In-3** are fungicidal in *C. albicans* with a survival rate of less than 1.5 % after 24 hours of compound exposure (Fig. 2 and Table S3, ESI). Taken together, the MIC and viability results here reveal that indium(III)-tpy complexes demonstrate significant antifungal activity in various *Candida* species for the first time.

2.3 Drug potential for indium compounds

Previously, the software SwissADME[26] has been used to identify potential drug candidates for chemical complexes containing transition metals.[27-29] Therefore, we used the SwissADME to analyse the physicochemical properties and assess the drug potential of **In-1**, **In-2** and **In-3** despite indium being a post-transition metal. The bioavailability radar hexagons for the three indium compounds
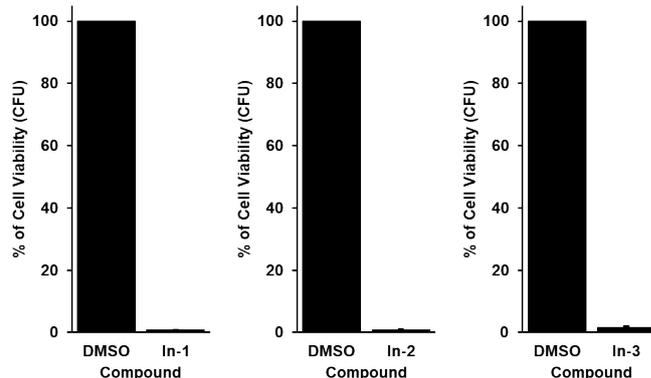

Fig. 2 Yeast viability assays. *C. albicans* SC5314 yeast cells were harvested following MIC assays, plated to nutrient YPD plates, and the average number of CFUs was determined from three technical replicates for each respective sample. The bar graphs depict the calculated cell viability percentage for cells treated with compounds **In-1**, **In-2** and **In-3** with a value of 100% survival assigned to the DMSO-treated yeast cell control group. See Table S3 (ESI) for data breakdown.

reveal similar physicochemical characteristics (Fig. 3 and Table S3, ESI). For instance, insolubility and saturation values fall outside the optimal ranges represented by the pink shaded region for all three complexes, while their flexibility and polarity values lie within or near the pink shaded regions of the hexagons. As expected, fluconazole satisfies five of the six categories, whereas caspofungin meets three of the criteria. Two criteria, flexibility and polarity, are favorable for the indium complexes **In-2** and **In-3**, while three criteria (size, flexibility, and polarity) are favorable for **In-1**. While the indium compounds **In-2** and **In-3** are larger than fluconazole and are unfavorable for oral bioavailability, they could potentially be developed into intravenous drugs, like the antifungal drug caspofungin. The size of complex **In-1** falls within the acceptable range for oral drugs, suggesting it could potentially be developed into an oral medication with further structural modifications. Structural adjustments to increase polarity, lower saturation and insolubility would be needed for all three complexes to reach drug-likeness. Thus, our findings validate the usage of SwissADME to evaluate complexes containing post-transition metals. Moreover, aside from antifungal observations with these complexes, alternative applications for these compounds should be explored with these advancements.
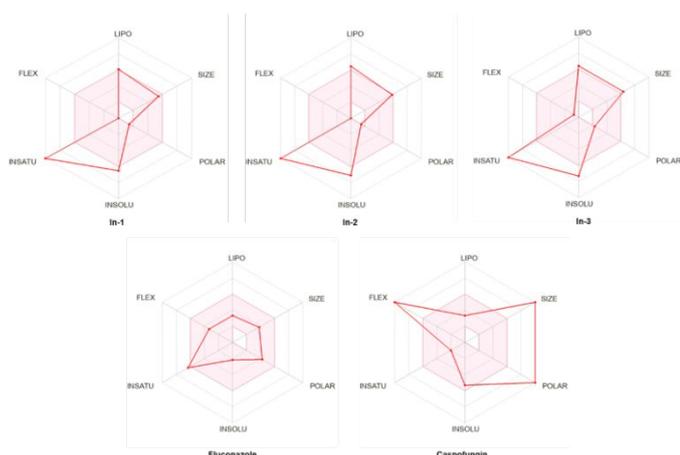
ARTICLE

Fig. 3 Physicochemical analyses of indium complexes (**In-1**, **In-2** and **In-3**), fluconazole, and caspofungin were conducted using SwissADME, an online tool that evaluates the drug potential of compounds based on characteristics of existing drugs.[26] The hexagonal plots display six key properties: lipophilicity, size, polarity, solubility, flexibility and saturation, with shaded areas indicating the desirable ranges for drug-like compounds. See Table S4 (ESI) for numerical values and range.

2.4 In-vitro anticancer activities

Next, the anti-cancer potency of these indium(III)-tpy compounds was tested and compared with that of the clinically approved drug cisplatin. The CCK-8 cell proliferation assay was used to evaluate the in vitro cytotoxicity of these indium(III)-tpy compounds against human breast cancer cells (MCF-7), triple-negative breast cancer cells (MDA-MB-468), and the non-tumorigenic mammary epithelial cell line (MCF-10A). The results obtained from cells treated with three indium compounds for 72 hours are summarized in Table 3. These compounds exhibit varying activities in inhibiting the growth of both cancerous and non-cancerous cells. All three compounds demonstrated promisingly low IC50 values against MCF-7 and MDA-MB-468 cells compared to cisplatin. However, they also exhibited inhibitory effects on the proliferation of the non-cancerous MCF-10A cells, particularly for **In-2**. Although **In-2** showed strong inhibition of cell proliferation, it was also highly toxic to non-cancerous cells, limiting its potential as a drug candidate. The other two compounds, **In-1** and **In-3**, demonstrated superior performance compared to **In-2**, positioning them as promising candidates for development as anticancer drugs. **In-1** exhibited relatively low toxicity toward the non-cancerous MCF-10A cells and the breast cancer MCF-7 cells, but it strongly inhibited the growth of the tumorigenic MDA-MB-468 cells, with an IC50 value as low as 0.336 ± 0.056 µM. In contrast, **In-3** showed relatively low toxicity toward MCF-10A cells but strongly

inhibited the growth of both MCF-7 and MDA-MB-468 tumorigenic cells, with IC50 values of 0.331 ± 0.089 µM and 0.363 ± 0.098 µM, respectively.

In addition, the stability of indium complexes in aqueous media as used for the cell treatment has been examined by the UV-Vis absorption spectroscopy. The water solutions of three compounds with a concentration of 1×10^{-5} M were obtained by diluting the stock solutions for each of the samples in DMSO, similar to the conditions used for cytotoxicity measurement. Their UV-Vis absorption spectra have been recorded for the samples both as prepared and after 72 h in the aqueous media (Fig. S4-S6, see ESI). The results reveal that drug candidates **In-1** and **In-2** are stable enough in aqueous solution for up to 72 h with only negligible changes in their UV-Vis absorption, while **In-3** experiences partial decomposition in water, probably owing to the hydrolysis of the complex.

Table 3 The 50% inhibitory concentrations (IC50, in µM) of compounds **In-1**, **In-2** and **In-3** against the non-tumorigenic epithelial cell lines MCF-10A, MCF-7, and MDA-MB 468 after 72 hours incubation.

	MCF-10A	MCF-7	MDA-MB 468
Cisplatin	18.70 ± 0.79	13.28 ± 1.82	3.35 ± 1.58
In-1	4.30 ± 1.22	4.01 ± 1.28	0.336 ± 0.056
In-2	0.932 ± 0.325	0.645 ± 0.170	1.03 ± 0.09
In-3	3.73 ± 1.80	0.331 ± 0.089	0.363 ± 0.098

3 Experimental

3.1 Materials and methods

Unless specified otherwise, the synthesis was carried out under ambient conditions. All chemicals of analytical grade are used as received from Thermo Fisher Scientific without further purification. Human breast cancer cell line (MCF-7), triple negative breast cancer cell line (MDA-MB-468) and non-tumorigenic epithelial cell line from mammary gland (MCF-10A) were obtained from the American Type Tissue Culture. All cell culture reagents were purchased from Thermo Fisher Scientific. FT-IR spectra were recorded on a Shimadzu 8400S instrument with solid samples under N_2 using a Golden Gate ATR accessory. UV-Vis electronic absorption spectroscopy was recorded on a Shimadzu UV-2700 spectrophotometer. Elemental analyses were performed by Midwest Microlab LLC in Indianapolis in the US.

3.2 Synthetic procedures

Synthesis of In-1. In a glovebox under N_2, in a 20 mL scintillation vial, 2,2';6',2''-terpyridine (L1, 233 mg, 1.00 mmol) and anhydrous $InCl_3$ (221 mg, 1.00 mmol) were added to THF (10 mL). The solution was allowed to stir at room temperature for 24 h, during which time a white suspension had formed. The precipitate was filtered and washed with THF (3 × 2 mL), dried in vacuo to give a white solid. Yield: 431 mg (95%). Colorless crystals of **In-1** were obtained by layering a methanolic $InCl_3$ solution onto a CH_2Cl_2-MeOH solution of L1 (1:1 M/L ratio) over 2 weeks and the X-ray diffraction analysis confirmed it was isostructural to that reported previously.[13]

Synthesis of In-2. A solution of 4'-chloro-2,2';6',2''-terpyridine (13.4 mg, 0.050 mmol) in MeOH/CH_2Cl_2 (10 mL, 1 : 3, v/v) was placed in a test tube. A blank solution of MeOH/CH_2Cl_2 (4 mL, 1: 1, v/v) was layered on the top of the ligand solution, followed by a solution of $InCl_3$ (11.0 mg, 0.050 mmol) in MeOH (8 mL). The tube was sealed and allowed to stand at room temperature for two weeks, after which time X-ray quality crystals of **In-2a** as brownish blocks have been collected, washed with MeOH and then dried in vacuo. Yield: 20 mg (82%). FT-IR (solid, cm^{-1}): 3004m, 1615m, 1595s, 1540s, 1478s, 1424m, 1405s, 1330m, 1306m, 1252s, 1166m, 1096m, 1073w, 1056w, 1022s, 994m, 895s, 812s, 794s, 732s, 627s. Anal. Calc. for $C_{15}H_{10}Cl_4InN_3$, C 36.85, H 2.06, N 8.60%; Found C 36.52, H 1.98, N 8.39%. For polymorph **In-2b**: A solution of 4'-chloro-2,2';6',2''-terpyridine (26.7 mg, 0.100 mmol) in MeOH/CH_2Cl_2 (10 mL, 1 : 3, v/v) was placed in a test tube. A blank solution of MeOH/CH_2Cl_2 (4 mL, 1: 1, v/v) was layered on the top of the ligand solution, followed by a solution of $InCl_3$ (22.0 mg, 0.100 mmol) in MeOH (8 mL). The tube was sealed and allowed to stand at room temperature for two weeks, after which time X-ray quality crystals of **In-2b** as colorless plates have been collected, washed with MeOH and then dried in vacuo. Yield: 37.5 mg (77%).

Synthesis of In-3. A solution of 4'-pyridyl-2,2';6',2''-terpyridine (31.0 mg, 0.100 mmol) in MeOH/CH_2Cl_2 (10 mL, 1 : 3, v/v) was placed in a test tube. A blank solution of MeOH/CH_2Cl_2 (4 mL, 1: 1, v/v) was layered on the top of the ligand solution, followed by a solution of $InCl_3$ (22.0 mg, 0.100 mmol) in MeOH (8 mL). The tube was sealed and allowed to stand at room temperature for 2 weeks, after which time X-ray quality crystals of **In-3** as pale-yellow needles have been collected, washed with MeOH and then dried in vacuo. Yield: 38.7 mg (73%). FT-IR (solid, cm^{-1}): 3064m, 1589s, 1556s, 1478s, 1420s, 1309w,

1251s, 1160w, 1127m, 1055m, 1021s, 881s, 829s, 789s, 726s, 687s, 656s, 643s. Anal. Calc. for $C_{20}H_{14}Cl_3InN_4$, C 45.19, H 2.65, N 10.54%; Found C 44.87, H 2.51, N 10.18%.

3.3 Antifungal Assays

3.3.1 Yeast strains and media

Minimum inhibitory concentration (MIC) assays. Yeast cells were collected form starter cultures and counted with a Countess 3 FL automated cell counter (Life Technologies, USA). Indium compounds were dissolved in DMSO to a final concentration of 5.0 mg/mL. Broth microdilution MIC assays were performed using a 96-well plate (Corning, USA) as previously described.[26] Briefly, indium compounds were serially diluted two-fold in a 100 µL volume of RPMI-1640 with a starting concentration of 128 µg/mL. Yeast cells were diluted approximately 1:100 in fresh RPMI-1640 medium, and 100 µL of cell suspension was added to each well to a final concentration of $1.0–3.0 × 10^5$ cells/mL. The final concentrations ranged from 0.125 to 64 µg/mL. Control wells containing cells that were grown in DMSO/RPMI-1640 or RPMI-1640 medium alone were prepared to evaluate the effect of DMSO or no compound on cell growth. Wells containing the compounds and RPMI-1640 medium without yeast cells were prepared to serve as a "blank" control. Yeast strains were grown for 24 hours at 30 °C with shaking, and OD_{600nm} readings were acquired every 30 min using a Synergy Mx plate reader (Biotek, USA). MIC values were obtained in broth dilution assays for yeast cells treated with the drug fluconazole (Sigma-Aldrich, USA) to validate yeast strain integrity and compare the antifungal activity of designated indium complex compounds against common antifungal drugs. For each assay, three technical replicates were analysed, and the mean and standard deviation for each OD_{600nm} reading was calculated using Microsoft Excel software. The results were confirmed in at least two independent experiments, and data presented is representative of one experiment.

3.3.2 Yeast viability assays

Yeast cells were harvested directly following the MIC assay and diluted 1:10,000 in distilled water. The cells were spread onto YPD plates, incubated for 2-3 days at 30°C, and colony forming units (CFUs) were counted. Selected indium compounds were tested in triplicate, and the mean and standard deviation of the

number of CFUs were determined for yeast cells treated with the designated indium compounds for 24 hours or DMSO (as a control group). The percentage of cell viability was determined via dividing the average number of CFUs from indium complex-treated cells by the average number of CFUs from DMSO-treated cells with the value of 100% being assigned to DMSO treated control groups. Viability assay results were confirmed in at least two independent experiments and data presented is representative of one experiment.

3.3.3 In silico analyses of indium complexes

The indium compounds were evaluated using an open-source tool, SwissADME, to predict their drug-likeness based on a library of existing drugs.[26] Indium compounds were input in the form of Simplified Molecular Input Line Entry System (SMILES). The results are displayed as a bioavailability radar. To compare the drug-likeliness properties of indium compounds, the antifungal drugs fluconazole and caspofungin were included in the analyses.

3.4 Cytotoxicity measurement

Three cell lines used for this study, the non-tumorigenic human mammary epithelial cell line (MCF-10A), the breast cancer cell line (MCF-7), and the triple-negative breast cancer cell line (MDA-MB 468), were obtained from ATCC. Cells were maintained in an incubator with 5% CO_2 at 37 ºC. The culture media of MCF-10A cells contained Dulbecco's modified Eagle's medium (DMEM) with 5% fetal bovine serum (FBS), 50 µg/mL gentamicin and a mixture of supplements: 10 µg/mL human insulin, 20 ng/mL hEGF, 100 ng/mL Cholera toxin, and 0.5 µg/mL hydrocortisone. The culture media of MCF-7 contained DMEM with 10% FBS and 50 µg/mL gentamicin. The culture media of MDA-MB-468 contained DMEM with 10% FBS, 2 mM L-glutamine and 50 µg/mL gentamicin. Cells were cultured into 96-well plates with a seeding density of $1×10^4$ cells per well to ensure that there is about 80% confluence when exposed to chemicals on the day prior to chemical treatment. A 100 mM stock solution for each compound was prepared by using dimethyl sulfoxide (DMSO) as a solvent. Chemical treatment solutions (0 to 100 µM) for each compound were then diluted from the stock solution in the culture media. The cytotoxicity was determined using CCK-8 cytotoxicity assay following the manufacturer's protocol (Sigma-Aldrich). The absorbance signals were detected by a BioTek Cytation 7 cell imaging

multimode reader at 450 nm. Three separate experiments were conducted for statistical analysis. IC50 was calculated using AAT Bioquest analysis (https://www.aatbio.com/tools/ic50-calculator (accessed on September 27, 2024)).

3.5 UV-Vis Absorption Spectroscopy

Solution samples of complexes **In-1**, **In-2** and **In-3** for the UV-Vis absorption measurements were prepared by the following procedure: a stock solution of each sample in DMSO (5 mL) was first prepared at a concentration of $1×10^{-3}$ M. A 50 µL solution was then taken and added to 5 mL of distilled water to give the final solution of $1×10^{-5}$ M for measurement. After the UV-Vis spectrum was recorded, the solution was kept at room temperature for 72 h and after which time the UV-Vis spectrum was recorded again.

3.6 X-ray Crystallography

X-ray diffraction data were collected on a Bruker D8 VENTURE diffractometer using Mo Kα radiation. Crystal data, data collection and refinement parameters are summarized in Table S1 (see ESI). The structures were solved using a dual-space method and standard difference map techniques and were refined by full-matrix least-squares procedures on F^2 with SHELXTL.[30,31] All hydrogen atoms bound to carbon were placed in calculated positions and refined with a riding model [U_{iso}(H) = 1.2–1.5U_{eq}(C)]. Hydrogen atoms bound to oxygen were located on the difference map and refined freely (**In-2a**) or with DFIX/DANG restraints [U_{iso}(H) = 1.2U_{eq}(O)] (**In-2b**). Potential MeOH disorder was explored for **In-2b**, but the disordered components were minor (10-20%) and did not refine well without additional significant restraints. CCDC Nos. 2378100-2378102 contain the supplementary crystallographic data for this paper. These data can be obtained free of charge via https://www.ccdc.cam.ac.uk/structures/, or from the Cambridge Crystallographic Data Centre, 12 Union Road, Cambridge CB2 1EZ, UK; fax: (+44) 1223-336-033; or e-mail: deposit@ccdc.cam.ac.uk.

4 Conclusions

In summary, we have synthesized three mononuclear indium(III) complexes (**In-1**, **In-2** and **In-3**) by using the tpy ligand and its 4′-Cl

and 4´-pyridyl derivatives, respectively. X-ray crystallographic analysis reveals that three complexes adopt the same coordination mode with a InN₃Cl₃ coordination sphere, and crystals of **In-2** were characterized as two different polymorphs. These indium(III)-tpy complexes were investigated for the first time for biological applications in order to understand their antifungal and anticancer behaviors. While all three indium compounds were observed to be fungicidal against the human fungal pathogen, *Candida albicans* and several non-albicans *Candida* species, **In-1**, was particularly promising for practical antifungal drug application. The cytotoxicity studies further demonstrate the potential of indium(III)-tpy complexes as antiproliferative agent against human breast cancer cells MCF-7 and MDA-MB 468.

Author contributions

S.-Y.C., J.R. and G.Z. conceived the project. X.C., Q.Z., A.K., H.K. and M.A. performed experimental studies and analysed the data. M.C.N. conducted the X-ray crystallographic analysis. All authors wrote and revised the manuscript.

Conflicts of interest

There are no conflicts to declare.

Data availability

Data supporting this article have been included as part of the ESI.† Crystallographic data have been deposited with Cambridge Crystallographic Data Centre under accession numbers 2378100-2378102.

Acknowledgements

Notes and references

1   B. Z. Momeni, N. Davarzani, J. Janczak, N. Ma and A. S. Abd-El-Aziz, Progress in design and applications of supramolecular assembly of 2, 2': 6', 2"-terpyridine-based first row d-block elements. *Coord. Chem. Rev.,* 2024, **506**, 215619.
2   R. R. Panicker and A. Sivaramakrishna, Remarkably flexible 2, 2': 6', 2"-terpyridines and their group 8–10 transition metal complexes–Chemistry and applications. *Coord. Chem. Rev.,* 2022, *459*, 214426.
3   J. Shi and M. Wang, Self-Assembly Methods for Recently Reported Discrete Supramolecular Structures Based on Terpyridine. *Chem.–An Asian J.* 2021, **16**, 4037.
4   A. Winter, Schubert, U.S. Metal-Terpyridine Complexes in Catalytic Application–A Spotlight on the Last Decade. *ChemCatChem*, 2020, **12**, 2890.
5   R. Abhijnakrishna, K. Magesh, A. Ayushi and S. Velmathi, Advances in the biological studies of metal-terpyridine complexes: an overview from 2012 to 2022. *Coord. Chem. Rev.* 2023, **496**, 215380.
6   R. Musiol, P. Malecki, M. Pacholczyk and J. Mularski, Terpyridines as promising antitumor agents: An overview of their discovery and development. *Exp. Opin. Drug Disc.* 2022, **17**, 259-271.
7   E. C. Constable, The coordination chemistry of 2, 2': 6', 2"-terpyridine and higher oligopyridines. *Adv. Inorg. Chem.*, 1986, **30**, 69.
8   S. F. Kainat, M. B. Hawsawi, E. U. Mughal, N. Naeem, A. M. Almohyawi, H. M. Altass, E. M. Hussein, A. Sadiq, Z. Moussa, A. S. Abd-El-Aziz and S. A. Ahmed, Recent developments in the synthesis and applications of terpyridine-based metal complexes: a systematic review. *RSC advances*, 2024, **14,** 21464.
9   M. Heller and U. S. Schubert, Syntheses of Functionalized 2, 2': 6', 2"-Terpyridines. *Eur. J. Org. Chem.*, 2003, **2003**, 947.
10   A. M. C., Thompson, The synthesis of 2, 2': 6', 2"-terpyridine ligands—versatile building blocks for supramolecular chemistry. *Coord. Chem. Rev.,* 1997, **160**, 1.
11   G. Zhang, H. Zeng, S. Zheng, M. C. Neary and P. A. Dub, Markovnikov alcohols via epoxide hydroboration by molecular alkali metal catalysts. *Iscience*, 2022, **25**, 105119.
12   G. Zhang, J. Wu, H. Zeng, M. C. Neary, M. Devany, S. Zheng and P. A. Dub, Dearomatization and functionalization of terpyridine ligands leading to unprecedented zwitterionic Meisenheimer aluminum complexes and their use in catalytic hydroboration. *ACS Catal.*, 2018, **9**, 874.
13   R. J. Butcher, C. George, N. Muratore and A. P. Purdy, Trichloro(2,6-di-2-pyridylpyridine-$\kappa^3 N$)indium(III). *Acta Cryst. Sec. E: Struct. Rep. Online*, 2003, **59**, m1107
14   R. Bhalla, W. Levason, S.K. Luthra, G. McRobbie, F. M. Monzittu, J. Palmer, G. Reid, G. Sanderson and W. Zhang, Hydrothermal synthesis of Group 13 metal trifluoride complexes with neutral N-donor ligands. *Dalton Trans.*, 2015, **44**, 9569.
15   A. J. Canty, L. A. Titcombe, B. W. Skelton and A. H. White, Synthesis and structural studies of dimethylindium (III) complexes with polydentate nitrogen donor ligands, and of monomethylindium (III) complexes containing alkoxide-bridged binuclear cations. *J. Chem. Soc., Dalton Trans.*, 1988, 35.
16   H. Beraldo, Pharmacological applications of non-radioactive indium (III) complexes: A field yet to be explored. *Coord. Chem. Rev.,* 2020, **419,** 213375.
17   A. B. de Carvalho, A. M. Souza, L. P. Bento, M. de Oliveira Silva, E. M. Souza-Fagundes, R. Diniz H. Beraldo, Indium (III) complexes with lapachol: cytotoxic effects against human breast tumor cells and interactions with DNA. *J. Bio. Inorg. Chem.*, 2024, **29**, 519.
18   W. Meza-Morales, Y. Alvarez-Ricardo, L. L. Pérez-González, R. Tavera-Hernández, M. T. Ramírez-Apan, R. A. Toscano, R. Sánchez-Obregón, M. A. Obregón-Mendoza and R. G. Enríquez, First Gallium and Indium Crystal Structures of Curcuminoid Homoleptic Complexes: All-Different Ligand Stereochemistry and Cytotoxic Potential. *Int. J. Mol. Sci.* 2023, **24**, 16324.
19   M. Jiang, Y. Chu, T. Yang, W. Li, Z. Zhang, H. Sun, H. Liang and F. Yang, Developing a novel indium (III) agent based on liposomes to overcome cisplatin-induced resistance in breast cancer by multitargeting the tumor microenvironment components. *J. Med. Chem.*, 2021, **64**, 14587.
20   T. O. Ajiboye, I. O. Amao, W. J. Adeyemi, S. O. Babalola, O. S. Akinsuyi, M. O. Ogunrombi, A. S. Ogunlaja and S. D. Mhlanga, Overview of medical and biological applications of indium(III) complexes. *Chem. Afr.*, 2024, **7**, 1729.

21 A. A. Oliveira, G. M. Perdigão, L. E. Rodrigues, J. G. da Silva, E. M. Souza-Fagundes, J. A. Takahashi, W.R. Rocha and H. Beraldo, Cytotoxic and antimicrobial effects of indium (III) complexes with 2-acetylpyridine-derived thiosemicarbazones. *Dalton Trans.*, 2017, **46**, 918.

22 K. Bajaj, R. M. Buchanan and C. A. Grapperhaus, Antifungal activity of thiosemicarbazones, bis (thiosemicarbazones), and their metal complexes. *J. Inorg. Biochem.*, 2021, **225**, 111620.

23 A. Winter, M. R. Gottschaldt, G. Newkome and U. S. Schubert, Terpyridines and their complexes with first row transition metal ions: Cytotoxicity, nuclease activity and self-assembly of biomacromolecules. *Curr. Top. Med. Chem.* 2012, **12**, 158-175.

24 S. Wu, Z. Wu, Q. Ge, X. Zheng, Z. Yang, Antitumor activity of tridentate pincer and related metal complexes. *Org. Biomol. Chem.* 2021, **19**, 5254.

25 K. A. Conrad, H. Kim, M. Qasim, A. Djehal, A. D. Hernday, L. Désaubry and J. M. Rauceo, Triazine-based small molecules: a potential new class of compounds in the antifungal toolbox. *Pathogens*, 2023, **12**, 126.

26 A. Daina, O. Michielin and V. Zoete, SwissADME: a free web tool to evaluate pharmacokinetics, drug-likeness and medicinal chemistry friendliness of small molecules. *Sci. Rep.*, 2017**, 7**, 42717.

27 K.J. Babu and D. Ayodhya, Comprehensive investigation of Co(II), Ni(II) and Cu(II) complexes derived from a novel Schiff base: Synthesis, characterization, DNA interactions, ADME profiling, molecular docking, and in-vitro biological evaluation. *Res. in Chem.*, 2023, **6**, 101110.

28 A. Arunadevi and N. Raman, Indole-derived water-soluble N, O bi-dentate ligand-based mononuclear transition metal complexes: In silico and in vitro biological screening, molecular docking and macromolecule interaction studies. *J. Biomol. Struct. Dyn*. 2020, **38**, 1499-1513.

29 J. Sączewski, Ł. Popenda and J. Fedorowicz, In Silico SwissADME Analysis of Antibacterial NHC–Silver Acetates and Halides Complexes. *Appl. Sci.*, 2024, **14**, 8865.

30 G. M. Sheldrick, SHELXTL, An Integrated System for Solving, Refining, and Displaying Crystal Structures from Diffraction Data; University of Göttingen, Göttingen, Federal Republic of Germany, 1981.

31 G. M. Sheldrick, SHELXT-Integrated Space-Group and Crystal-Structure Determination. *Acta Cryst.* 2015, **A71**, 3-8.

Data availability statement

Data supporting this article have been included as part of the ESI. Crystallographic data have been deposited with Cambridge Crystallographic Data Centre under accession numbers 2378100-2378102.